Fabrication and Dispersion of Gold-Shell-Protected Magnetite Nanoparticles: Systematic Control Using Polyethyleneimine

Ian Y. Goon,[†] Leo M. H. Lai,[‡] May Lim,[†] Paul Munroe,[§] J. Justin Gooding,[‡] and Rose Amal[†,*]

ARC Centre of Excellence for Functional Nanomaterials, School of Chemical Sciences and Engineering, School of Chemistry and Electron Microscope Unit, University of New South Wales, Sydney NSW 2052 Australia

Received September 17, 2008. Revised Manuscript Received December 18, 2008

A detailed study of the aqueous synthesis of composite 50−150 nm magnetite−gold core−shell nanoparticles with the ability to engineer the coverage of gold on the magnetite particle surface is presented. This method utilizes polyethyleneimine for the dual functions of attaching 2 nm gold nanoparticle seeds onto magnetite particles as well as preventing the formation of large aggregates. Saturation of the magnetite surface with gold seeds facilitates the subsequent overlaying of gold to form magnetically responsive core−shell particles, which exhibit surface plasmon resonance. In-depth characterization and quantification of the gold-shell formation process was performed using transmission electron microscopy, X-ray photoelectron spectroscopy, energy-dispersive spectroscopy, and inductively coupled plasma optical emission spectroscopy. Dynamic light scattering studies also showed that PEI coating of synthesized particles served as an excellent barrier against aggregation. The ability of the gold shell to protect the magnetite cores was tested by subjecting the particles to a magnetite-specific dissolution procedure. Elemental analysis of dissolved species revealed that the gold coating of magnetite cores imparts remarkable resistance to iron dissolution. The ability to engineer gold coverage on particle surfaces allows for controlled biofunctionalization, whereas their resistance to dissolution ensures applicability in harsh environments.

Introduction

Magnetic iron oxide nanoparticles have recently become the focus of a considerable amount of research activity in biomedicine.[1] Magnetite (Fe_3O_4) nanoparticles, in particular, are attractive because of their high magnetic moment, nontoxic nature, and ease of synthesis.[2] Several applications in which the properties of magnetite are envisaged as useful include biological detection and imaging,[3] targeted drug delivery,[4] and gene therapy.[5,6] In addition to their magnetic properties, the biomedical applicability of nanoscale magnetite particles is dependent upon their stability against aggregation in physiological environments, and the ability to predictably functionalize the particle surface for specific biomolecule interactions.[1] Because of their large surface area to volume ratio and low surface charge at neutral pH,[7] magnetite nanoparticles tend to aggregate in physiological environments. This, coupled with the lack of predictable methods for specific functionalization of magnetite surfaces with biomolecules,[1] has led to studies that attempt to improve the aggregation stability and surface functionality by modifying the oxide surface with gold.[8−16] Gold is the material of choice because of its chemical stability and biocompatibility,[17] as well as its established reactivity with thiolated compounds. The latter allows facile, predictable function-

* Corresponding author. Tel.: 61 2 9385 4361. Fax: 61 2 9385 5966. E-mail: r.amal@unsw.edu.au.

[†] School of Chemical Sciences and Engineering, University of New South Wales.

[‡] School of Chemistry, University of New South Wales.

[§] Electron Microscope Unit, University of New South Wales.

(1) Gupta, A. K.; Gupta, M. *Biomaterials* **2005**, *26* (18), 3995–4021.
(2) Schwertmann, U.; Cornell, R. M. *Iron Oxides in the Laboratory: Preparation and Characterization*, 2nd ed.; Wiley-VCH: Weinheim, Germany, 2000; p 204.
(3) Lee, J.-H.; Huh, Y.-M.; Jun, Y.-w.; Seo, J.-w.; Jang, J.-t.; Song, H.-T.; Kim, S.; Cho, E.-J.; Yoon, H.-G.; Suh, J.-S.; Cheon, J. *Nat. Med.* **2007**, *13* (1), 95–99.
(4) Dobson, J. *Drug Dev. Res.* **2006**, *67* (1), 55–60.
(5) Li, D.; Teoh, W. Y.; Selomulya, C.; Woodward, R. C.; Amal, R.; Rosche, B. *Chem. Mater.* **2006**, *18* (26), 6403–6413.
(6) Scherer, F.; Anton, M.; Schillinger, U.; Henke, J.; Bergemann, C.; Krüger, A.; Gänsbacher, B.; Plank, C. *Gene Ther.* **2002**, *9* (2), 102–109.
(7) Illes, E.; Tombacz, E. *J. Colloid Interface Sci.* **2006**, *295* (1), 115–123.
(8) Lyon, J. L.; Fleming, D. A.; Stone, M. B.; Schiffer, P.; Williams, M. E. *Nano Lett.* **2004**, *4* (4), 719–723.
(9) Lo, C. K.; Xiao, D.; Choi, M. M. F. *J. Mater. Chem.* **2007**, *17* (23), 2418–2427.
(10) Wang, L.; Luo, J.; Maye, M. M.; Fan, Q.; Rendeng, Q.; Engelhard, M. H.; Wang, C.; Lin, Y.; Zhong, C.-J. *J. Mater. Chem.* **2005**, *15* (18), 1821–1832.
(11) Wang, L.; Luo, J.; Fan, Q.; Suzuki, M.; Suzuki, I. S.; Engelhard, M. H.; Lin, Y.; Kim, N.; Wang, J. Q.; Zhong, C.-J. *J. Phys. Chem. B* **2005**, *109* (46), 21593–21601.
(12) Xu, Z.; Hou, Y.; Sun, S. *J. Am. Chem. Soc.* **2007**, *129* (28), 8698–8699.
(13) Mikhaylova, M.; Kim, D. K.; Bobrysheva, N.; Osmolowsky, M.; Semenov, V.; Tsakalakos, T.; Muhammed, M. *Langmuir* **2004**, *20* (6), 2472–2477.
(14) Mandal, M.; Kundu, S.; Ghosh, S. K.; Panigrahi, S.; Sau, T. K.; Yusuf, S. M.; Pal, T. *J. Colloid Interface Sci.* **2005**, *286* (1), 187–194.
(15) Spasova, M.; Salgueirino-Maceira, V.; Schlachter, A.; Hilgendorff, M.; Giersig, M.; Liz-Marzan, L. M.; Farle, M. *J. Mater. Chem.* **2005**, *15* (21), 2095–2098.
(16) Lim, J.; Eggeman, A.; Lanni, F.; Tilton, R. D.; Majetich, S. A. *Adv. Mater.* **2008**, *20* (9), 1721–1726.
(17) Shukla, R.; Bansal, V.; Chaudhary, M.; Basu, A.; Bhonde, R. R.; Sastry, M. *Langmuir* **2005**, *21* (23), 10644–10654.

10.1021/cm8025329 CCC: $40.75
Published on Web 01/22/2009

alization of the particles with the aim of stabilizing particles against aggregation and adding biological functionality.[18]

Synthesis of magnetite particles coated completely with gold involves two main processes of magnetite nanoparticle core synthesis and the subsequent coating with a layer of gold. Methods of obtaining gold-coated magnetite can be categorized according to the variations in each of the two processes. Initial attempts to coat magnetite with gold involved the use of reverse micelles as constrained reactors for both particle synthesis and gold coating.[13,14] Such reverse micelle methods are able to form gold-coated particles but are of low yield and are fairly difficult to reproduce.[19] The second category involves both synthesis and coating in aqueous phase,[8,9] whereby magnetite nanoparticles are synthesized by the precipitation of iron salts in an alkaline environment followed by the reduction of chloroauric acid to form a gold coating. These aqueous methods are simple and quick and produce particles that are dispersible in water. The particle aggregate size and gold-shell thickness, however, is difficult to control, and synthesized samples contain a mixture of coated and uncoated magnetite that has proven problematic to separate. A third category of methods consist of magnetite synthesis and gold coating in organic phase.[10,11] Such methods involve the thermal decomposition of iron(III) oleate to magnetite nanoparticles followed by coating via reduction of gold acetate in the presence of capping agents. Organic methods usually result in significantly enhanced particle size and shell thickness control with excellent resistance to aggregation in organic solvents. The particles, at least in our studies, are weak in responding to magnetic field and aggregated when the phase was transferred into aqueous environment. These organic methods also use nongreen solvents and may prove difficult to scale up. To achieve size control and viability in aqueous environment, a fourth category of synthesis methods has emerged more recently involving a combination of organic synthesis of magnetite cores followed by gold coating of particles in an aqueous environment.[12,16] The reported methods appear to be capable of producing particles with well-controlled primary particle sizes, but the extent to which the particles are fully coated and remain stable to aggregation remains unexplored.

A separate class of gold−magnetite composites has also been reported involving the attachment of discrete gold nanoparticles onto magnetite without forming a full coating.[20−22] Such composites may be useful in applications such as protein separation, optical imaging or catalysis, where a full coating is not necessarily required. These composites can be synthesized by several methods including attaching functional molecules with amine or thiol groups onto magnetite nanoparticles, which then allows for covalent attachment of gold nanoparticles, [20,21] or energetic attachment via γ-ray irradiation.[22] These methods, however, have not shown the ability to systematically control the gold nanoparticle loading onto the magnetite surface, as well as the extent to which the particles are stable against aggregation. Such particles without a full gold coating are also limited to use in environments where leaching or degradation of the exposed magnetite core does not occur.

An important requirement for the widespread use of iron oxide composites is the ability to keep the synthesized particles stable against aggregation under conditions similar to those of the intended application. Aggregation stability is particularly important for in vivo biomedical applications in which aggregation could cause unwanted accumulation of particles or blood vessel blockage. Primary particle size[23] and surface functionalization[23] along with the pH[24,25] and ionic strength[26] of the solution have been reported to affect iron oxide colloidal stability; however, previously reported methods of synthesizing Au−Fe_3O_4 composites do not address particle aggregation stability in detail.

In this paper, we report a facile method of synthesizing 50−150 nm magnetite-gold composites via the use of a biocompatible polyelectrolyte, polyethyleneimine (PEI),[27] for the dual function of attaching gold seeds and preventing the formation of large aggregates. We show that successful gold coating of magnetite requires the self-assembly of a layer of PEI onto magnetite cores and subsequent saturation of the surface with 2 nm gold seeds. We demonstrate that the magnetite cores are coated with a protective layer of gold, which is resistant to chemical attack of the magnetite core and also show the ability of PEI to increase particle stability against aggregation, both of which are important for further application of the synthesized particles.

Experimental Section

Materials. Polyethyleneimine (PEI, branched, $M_w \approx 25\,000$ g mol^{-1}), sodium borohydride ($NaBH_4$), sodium citrate ($C_6H_5Na_3O_7 \cdot H_2O$), nitric acid (HNO_3), and chloroauric acid ($HAuCl_4$) were obtained from Sigma-Aldrich (Sydney, Australia). Iron(II) sulfate ($FeSO_4$), potassium nitrate (KNO_3), hydrochloric acid (HCl), sodium hydroxide (NaOH), ammonium oxalate ($(NH_4)_2C_2O_4 \cdot H_2O$)), and oxalic acid ($HO_2C_2O_2H$) were obtained from Ajax Chemicals (Sydney, Australia). Hydroxylamine hydrochloride ($NH_2OH \cdot HCl$) was obtained from Fluka (Sydney, Australia). All chemicals were used as received with no further purification.

Synthesis of 50 nm PEI-Functionalized Fe_3O_4 Cores (Fe_3O_4−PEI). The 50 nm (average face-centered diagonal) cubic Fe_3O_4 cores (Figure 1a) were precipitated by mixing 0.7 g of $FeSO_4$ with 80 mL of distilled water followed by the addition of 10 mL of 2.0 M KNO_3 and 10 mL of 1.0 M NaOH and in an oxygen-free

(18) Brust, M.; Walker, M.; Bethell, D.; Schiffrin, D. J.; Whyman, R. *J. Chem. Soc., Chem. Commun.* **1994**, 801–802.
(19) Lee, Y.; Lee, J.; Bae, C. J.; Park, J. G.; Noh, H. J.; Park, J. H.; Hyeon, T. *Adv. Funct. Mater.* **2005**, *15* (3), 503–509.
(20) Caruntu, D.; Cushing, B. L.; Caruntu, G.; O'Connor, C. J. *Chem. Mater.* **2005**, *17* (13), 3398–3402.
(21) Bao, J.; Chen, W.; Liu, T.; Zhu, Y.; Jin, P.; Wang, L.; Liu, J.; Wei, Y.; Li, Y. *ACS Nano* **2007**, *1* (4), 293–298.
(22) Seino, S.; Kinoshita, T.; Otome, Y.; Nakagawa, T.; Okitsu, K.; Mizukoshi, Y.; Nakayama, T.; Sekino, T.; Niihara, K.; Yamamoto, T. A. *J. Magn. Magn. Mater.* **2005**, *293* (1), 144–150.
(23) Portet, D.; Denizot, B.; Rump, E.; Lejeune, J.-J.; Jallet, P. *J. Colloid Interface Sci.* **2001**, *238* (1), 37–42.
(24) Amal, R.; Raper, J. A.; Waite, T. D. *J. Colloid Interface Sci.* **1992**, *151* (1), 244–257.
(25) Tombácz, E.; Csanaky, C.; Illés, E. *Colloid Polym. Sci.* **2001**, *279* (5), 484–492.
(26) Amal, R.; Coury, J. R.; Raper, J. A.; Walsh, W. P.; Waite, T. D. *Colloids Surf.* **1990**, *46* (1), 1–19.
(27) Boussif, O.; Lezoualc'h, F.; Zanta, M. A.; Mergny, M. D.; Scherman, D.; Demeneix, B.; Behr, J. *Proc. Nat. Acad. Sci. U.S.A.* **1995**, *92* (16), 7297–7301.

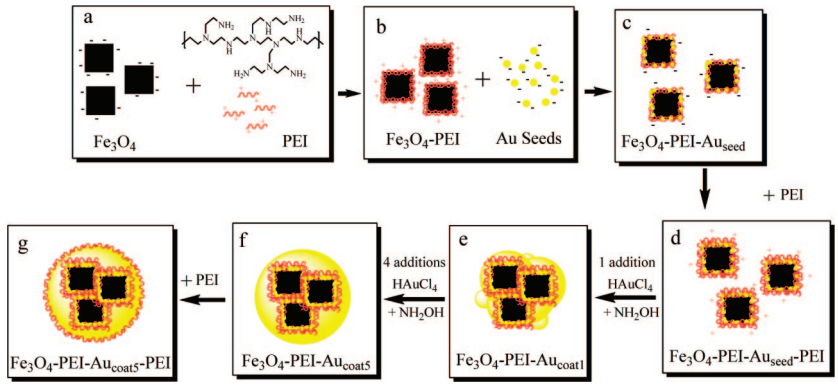

Figure 1. Schematic representation of the synthesis of gold−magnetite core−shell particles. (a) Cationic polyethyleneimine (PEI) self-assembled onto negatively charged magnetite (Fe_3O_4). (b) Fe_3O_4−PEI mixed with Au seeds, to obtain (c) Au-seeded Fe_3O_4, after which PEI is again added to obtain (d) PEI-coated Au-seeded Fe_3O_4. (e) One addition of $HAuCl_4$ and NH_2OH results in an uneven gold shell. (f) Four subsequent additions of $HAuCl_4$ and NH_2OH PEI form an even gold coating. (g) PEI is then added to increase stability against aggregation.

environment.[28] The initially formed $Fe(OH)_2$ was heated at 90 °C in the presence of varying concentrations of PEI solution (0 to 4 g/L) for 2 h, during which $Fe(OH)_2$ was oxidized to Fe_3O_4 nanoparticles with PEI self-assembled on its surface (Figure 1b). Particles were magnetically separated from reaction mixture by placing a neodymium disk magnet (25 mm diameter) magnet below the reaction vessel (200 mL beaker) for 5 min to capture all magnetic particles before discarding the reaction solution. The collected Fe_3O_4−PEI particles were rinsed 5 times with Milli-Q water and suspended in 80 mL of Milli-Q water, yielding a suspension of Fe_3O_4 (3.2 g/L, pH 7).

Synthesis of Au-Seeded Fe_3O_4 Nanoparticles (Fe_3O_4−PEI−Au_{seed}). A 2 mL volume of the above Fe_3O_4−PEI suspension was first sonicated for 2 min with an ultrasonic probe (Misonix S3000 Sonicator) and then stirred for 2 h with 90 mL of 2 nm colloidal gold particles. The colloidal gold particles were produced from the $NaBH_4$ (0.075%) reduction of 1% $HAuCl_4$ in 38.8 mM sodium citrate.[29] The Fe_3O_4−PEI−Au_{seed} particles (Figure 1c) were magnetically separated from excess Au colloid solution and rinsed 5 times with Milli-Q water. The particle surfaces were then functionalized again with PEI by heating in a 60 °C oven for 1 h in the presence of a 5 g/L PEI solution followed by rinsing 5 times and dispersion in 20 mL of Milli-Q water with an ultrasonic probe.

Synthesis of Au-Coated Fe_3O_4 Nanoparticles (Fe_3O_4−PEI-Au_{coat}). Au shells were next grown by iterative reduction of $HAuCl_4$ onto the Fe_3O_4−PEI-Au_{seed}−PEI.[8,29] Twenty milliliters of Au-seeded Fe_3O_4 was mechanically stirred with 110 mL of 0.01 M NaOH (pH ~11.5). A first iteration of 0.5 mL of 1% $HAuCl_4$ was added along with 0.75 mL of 0.2 M NH_2OH.HCl followed by 0.5 mL of 1% $HAuCl_4$ and 0.25 mL of 0.2 M NH_2OH.HCl for the subsequent iterations. A total of up to five iterations were made, with 10 min in between iterations. The Fe_3O_4−PEI−Au_{coat5} (Figure 1f) particles were then magnetically separated from the reaction mixture, rinsed 5 times, and dispersed in 20 mL of Milli-Q water with an ultrasonic probe.

Oxalate Dissolution of Uncoated Fe_3O_4. Two-hundred milliliters of a pH 3, 0.02 M oxalate solution was prepared by mixing 0.284 g of ammonium oxalate and 0.252 g of oxalic acid. Three 10 mL portions of each type of particle (Fe_3O_4, Fe_3O_4−PEI−Au_{seed}, and Fe_3O_4−PEI−Au_{coat5}) (9 samples in total) were added to individual sample tubes and magnetically separated from solution. Twenty milliliters of oxalate solution was then added to each sample tube, and each set of tubes was mixed with a mechanical spinner for either 1, 24, or 168 h. Control samples were made by taking a 10 mL portion of each type of particle, magnetically separating the particles from solution and dissolving them completely in 20 mL of aqua regia.

Characterization. Transmission electron microscopy (TEM) and energy-dispersive spectroscopy (EDS) elemental maps were used to study the crystal lattice patterns and particle core−shell structure using a Philips CM 200 TEM operating at 200 kV. ζ-potential measurements to characterize the particle surface charge and its effect on aggregation were obtained using a Brookhaven ZetaPALS ζ-potential analyzer. Particle size distributions were obtained based on dynamic light scattering (DLS) principles with a Brookhaven 90 Plus particle sizer. UV−visible absorption spectra were obtained with a Cary 300 UV−vis spectrophotometer to detect surface plasmon resonance (SPR) on the coated particles. Total organic carbon (TOC) measurements to determine PEI concentrations were performed by a Shimadzu TOC-VCSH analyzer. Magnetization curves and saturation magnetization values of the magnetite particles at various stages of the process were measured using an MPMS-5T superconducting quantum interference device (SQUID) magnetometer at 25 °C. The compositions of the coated magnetite particles were measured using an Optima 3000D Inductively coupled plasma (ICP-OES) optical emission spectrometer. Changes in particle surface compositions as Au was immobilized onto Fe_3O_4 was characterized via X-ray photoelectron spectroscopy (XPS) on a Thermo Scientific VG-ESCALAB 220-iXL spectrometer with a monochromated Al Kα source (1486.6 eV). The spectra were accumulated at a takeoff angle of 90° and analyzer pass energy of 20 eV.

Results and Discussion

Controlled Loading of PEI on Fe_3O_4 (Fe_3O_4−PEI). The first step in this synthesis method involved the immobilization of the polycation, PEI on the Fe_3O_4 particles (Figure 1a). The addition of PEI during the synthesis of Fe_3O_4 nanoparticles was found to be an effective method of systematically controlling the amount of PEI attached to Fe_3O_4. During the formation of Fe_3O_4 particles at pH 11, the positively charged PEI in the reaction solution binds to the negatively charged Fe_3O_4 via electrostatic self-assembly[30] to form a stabilizing polyelectrolyte layer, clearly identified using HRTEM, as indicated by the

(28) Sugimoto, T.; Matijevic, E. *J. Colloid Interface Sci.* **1980**, *74* (1), 227–243.
(29) Brown, K. R.; Walter, D. G.; Natan, M. J. *Chem. Mater.* **2000**, *12* (2), 306–313.
(30) Berret, J. F.; Schonbeck, N.; Gazeau, F.; ElKharrat, D.; Sandre, O.; Vacher, A.; Airiau, M. *J. Am. Chem. Soc.* **2006**, *128* (5), 1755–1761.

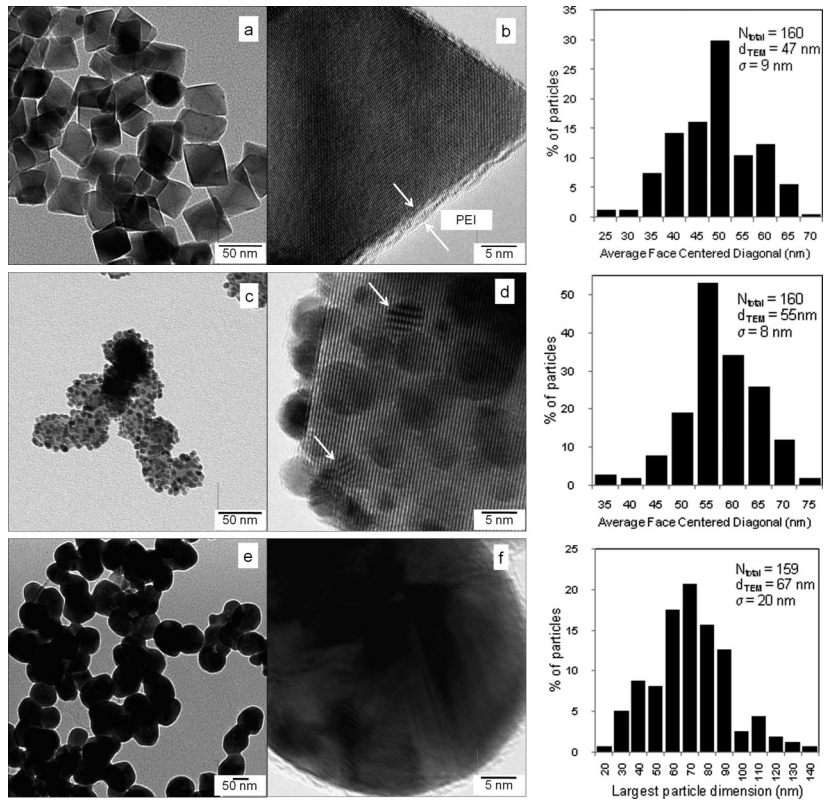

Figure 2. (a) TEM image of Fe_3O_4−PEI cores; (b) HRTEM image of a Fe_3O_4−PEI particle; (c) TEM image of Fe_3O_4−PEI−Au_{seed} cores; (d) HRTEM image of a Fe_3O_4−PEI−Au_{seed} particle; (e) TEM image of Fe_3O_4−PEI−Au_{coat5}−PEI; (f) high-magnification TEM image of a Fe_3O_4−PEI−Au_{coat5}−PEI particle.

Table 1. PEI Adsorption on Fe_3O_4 by TOC Measurements and Compositions of Au-seeded−Fe_3O_4 Composites by ICP-OES

PEI adsorbed (μg cm^{-2})	Au (wt %)	Fe_3O_4 (wt %)	Au (vol %)	Fe_3O_4 (vol %)
0.00	0.0	100.0	0.0	100.0
0.06	5.0	95.0	1.4	98.6
0.49	27.5	72.5	9.2	90.8
0.75	35.5	64.5	12.8	87.2
0.87	43.0	57.0	16.8	83.2
0.89	47.7	52.3	19.6	80.4

arrows in Figure 2b. The amount of PEI adsorbed onto the particles was determined by measuring the solution organic carbon content (via TOC measurements), after PEI was adsorbed onto Fe_3O_4, and then comparing this to the organic carbon concentration of control samples not containing Fe_3O_4 particles. The maximum amount of PEI adsorbed was calculated to be 0.88 μg PEI per cm^2 particle surface (assuming 50 nm cubic F_3O_4 particles) (Table. 1). The effect of increasing the amount of PEI on the particle zeta potential is presented in Figure 3, determined from electrophoretic mobility measurements in 10 mM NaCl background electrolyte, pH 7. Effective particle diameter measurements obtained via dynamic light scattering (also in Figure 3) indicates that increasing the PEI on Fe_3O_4 surfaces decreases the effective particle aggregate size. This can be attributed to the increasing electrostatic repulsion between particles as well as steric hindrance provided by increasing the particle surface polymer concentration.

The electrostatic adsorption of polyelectrolytes onto oppositely charged particles has been found to be dependent

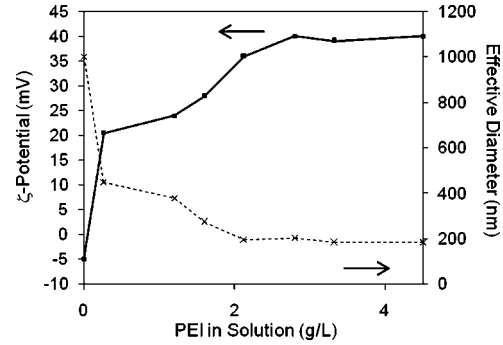

Figure 3. ζ-potentials and effective diameter of Fe_3O_4 loaded with different amounts of PEI with 10 mM NaCl background electrolyte, pH 7.

on polyelectrolyte chain length and particle size.[31,32] For the 50 nm Fe_3O_4 cores synthesized by this method, PEI with a molecular weight of ~25 000 g mol^{-1} was found to provide the greatest stability against aggregation, (when compared to PEI with molecular weights of ~800 and ~600 000 g mol^{-1} (see Figure S1 in the Supporting Information)). We propose that for a given particle size, that certain polymer lengths/molecular weights are ideal for stabilization of particles from aggregation.[31,33] Suspensions of Fe_3O_4−PEI remained resistant to aggregation and settling for the 30 day period over which the study was undertaken, compared to a matter of minutes without PEI, demonstrating the advantage of a PEI layer on Fe_3O_4 as a barrier to aggregation.

(31) Mayya, K. S.; Schoeler, B.; Caruso, F. *Adv. Funct. Mater.* **2003**, *13* (3), 183–188.
(32) Schneider, G.; Decher, G. *Langmuir* **2008**, *24* (5), 1778–1789.
(33) Gittins, D. I.; Caruso, F. *J. Phys. Chem. B* **2001**, *105* (29), 6846–6852.

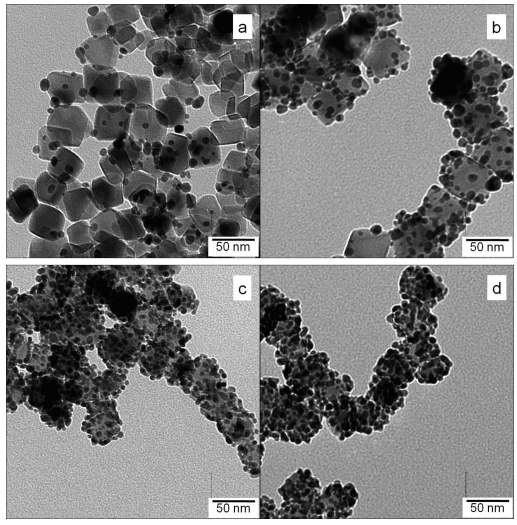

Figure 4. TEM images of Fe_3O_4 with (a) 0.06, (b) 0.49, (c) 0.75, and (d) 0.89 μg/cm^2 PEI adsorbed after 2 h of mixing with Au seed nanoparticles.

Controlled Attachment of Au Seeds on Fe_3O_4 (Fe_3O_4−PEI−Au_{seed}). In addition to controlling aggregate size, the ability to systematically control amounts of PEI on Fe_3O_4 allows for controlled attachment of negatively charged Au seeds to the Fe_3O_4 nanoparticles via electrostatic and weak covalent bonding with amines on PEI (images b and c in Figure 1).[34] Figure 2c shows a uniform spread of 2 nm Au seed particles attached onto Fe_3O_4−PEI cores after 2 h of mixing, close inspection of the HRTEM image of a single particle in Figure 2d reveals the difference in lattice fringes between the Au seeds (indicated with arrows) and Fe_3O_4 cores, which provides strong evidence of the composite nature of the particle. Qualitative evidence of controlled Au loading is observed in a series TEM images in Figure 4a to 4d, showing increasing particle surface coverage with Au seeds as a result of increased PEI concentration on the Fe_3O_4. These findings are supported quantitatively by ICP-OES measurements of the Fe_3O_4−PEI−Au_{seed} composites (dissolved in aqua regia), which provide the Au and Fe_3O_4 compositions (Table 1) of the particles in the respective images in Figure 4. The Au to Fe_3O_4 ratios obtained indicate an increased amount of immobilized Au seed particles on Fe_3O_4 surface as a result of the greater amount of NH_2 groups provided by the PEI. The difference in density of Au (19.3 g/cm^3) and Fe_3O_4 (5.15 g/cm^3)[2] accounts for the difference in % weight and % volume numbers.

These results highlight the utility of PEI as a functional layer that allows systematic control of Au loading. Fe_3O_4 particles saturated with PEI can be used to produce composites with a greater Au seed density when compared to other methods in literature.[20,21] The ability to control Au loading on Fe_3O_4 is also important when considering other applications where a complete Au shell is not required such as catalysis,[35] and protein separation,[21] where the amount of Au on the particle affects the magnitude of binding with biofunctionalizing molecules. Further mention of Fe_3O_4−PEI-Au_{seed} particles in this article refers to Fe_3O_4 cores with the maximum (0.89 μg/cm^2) amount of PEI adsorbed on the surface.

Formation of Fe_3O_4−Au Core−Shell Particles (Fe_3O_4−PEI−Au_{coat}). Growth of a complete Au shell around the Fe_3O_4−PEI−Au_{seed} particles required the deposition of more Au on the particle surface (Figure 1d−f). The iterative reduction of $HAuCl_4$ in the presence of Fe_3O_4−PEI−Au_{seed} using $NH_2OH\cdot HCl$ was selected for this purpose because the method is simple and rapid. The iterative growth of the Au shell was monitored via TEM micrographs (Figure 5). In Figure 5a, after one addition, the Au seed particles were visibly larger and beginning to coalesce, whereas in images b and c Figure 5, after three and four additions, the initial seed particles merge and became almost indistinguishable with an uneven shell forming. In Figure 5d, after five additions, a discrete and even Au coating was observed, with particle sizes ranging between 40 and 110 nm (Figure 2e), indicating the likely presence in some cases of multiple Fe_3O_4 cores within a single Au-coated Fe_3O_4 particle. We estimate that for the Fe_3O_4−PEI−Au_{coat5} particles, approximately 53% contain 1 Fe_3O_4 core particle, 30% contain 2 Fe_3O_4 core particles, 12% contain 3 Fe_3O_4 core particles, and 5% contain 4 Fe_3O_4 core particles (details of estimations in S3 in the Supporting Information). The high-magnification TEM image of a coated particle after five additions in Figure 2f indicates the dense nature of the Au coating, which prevents the observation of lattice structures, which were clearly visible prior to coating. ICP-OES analysis of the Au and Fe_3O_4 compositions after each iteration (Table 2) revealed a 30 wt % increase in Au after the first iteration followed by smaller increases for subsequent iterations. The large initial increase was attributed to the presence of PEI on the Fe_3O_4−PEI−Au_{seed}, surface which aids the initial deposition and growth of the Au shell.

A dense layer of attached Au seeds on the Fe_3O_4 surface was found to play an important role in ensuring that all the initial bare Fe_3O_4 particles were coated with Au. Attempts to coat Fe_3O_4−PEI particles without, or with only a small number of attached Au seeds, resulted in a majority of the Fe_3O_4 remaining uncoated (see Figure S1 in the Supporting Information). The dense layer of Au seeds is important because it provides a large number of evenly spread nucleation sites on the Fe_3O_4 particles which encourages a more uniform distribution of Au deposition during the coating iterations. Also, the reduction of Au^{3+} to Au^0 using NH_2OH has been shown to be significantly catalyzed by Au surfaces,[36] which means that the lack of sufficient Au seed particles on Fe_3O_4 surfaces is likely to result in the growth of an Au shell on some particles and not others.

The use of this method for obtaining Au-coated Fe_3O_4 ensures that all particles have Au attached. One issue, however, is that the synthesized particles are not monodispersed. This appears to be a common issue to a varying extent

(34) Leff, D. V.; Brandt, L.; Heath, J. R. *Langmuir* **1996**, *12* (20), 4723–4730.
(35) Kydd, R.; Chiang, K.; Scott, J.; Amal, R. *Photochem. Photobiol. Sci.* **2007**, *6* (8), 829–832.
(36) Stremsdoerfer, G.; Perrot, H.; Martin, J. R.; Clechet, P. *J. Electrochem. Soc.* **1988**, *135* (11), 2881–2886.

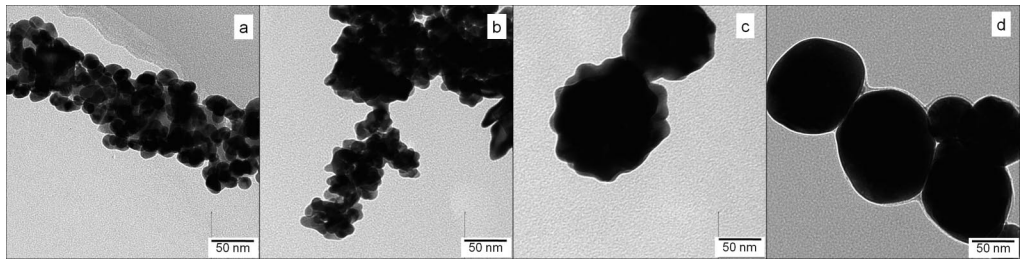

Figure 5. TEM images of Au-coated Fe_3O_4 after (a) one iteration of $Fe_3O_4-PEI-Au_{coat1}$; (b) three iterations of $Fe_3O_4-PEI-Au_{coat3}$; (c) four iterations of $Fe_3O_4-PEI-Au_{coat4}$; and (d) five iterations of $Fe_3O_4-PEI-Au_{coat5}$.

Table 2. ICP-OES Compositions of Au-Coated Fe_3O_4

sample	no. of iterations	Au (wt %)	Fe_3O_4 (wt %)	Au (vol %)	Fe_3O_4 (vol %)
$Fe_3O_4-PEI-Au_{seed}$	0	44.7	55.3	17.8	82.2
$Fe_3O_4-PEI-Au_{coat1}$	1	74.2	25.8	43.4	56.6
$Fe_3O_4-PEI-Au_{coat2}$	2	77.7	22.3	48.2	51.8
$Fe_3O_4-PEI-Au_{coat3}$	3	83.1	16.9	56.8	43.2
$Fe_3O_4-PEI-Au_{coat4}$	4	91.2	8.8	73.5	26.5
$Fe_3O_4-PEI-Au_{coat5}$	5	92.6	7.4	77.1	22.9

Table 3. ICP-OES Elemental Analysis Demonstrating the Selective Oxalate Dissolution of Magnetite

sample	time elapsed (h)	solution	gold conc (mg/L)	iron conc (mg/L)	% iron dissolved
Fe_3O_4	control	aqua regia	0	81.90	100.0
	1	OA/AO	0	82.95	100.0
	24	OA/AO	0	81.45	100.0
$Fe_3O_4-PEI-Au_{seed}$	control	aqua regia	101.52	88.83	100.0
	1	OA/AO	0	0.36	0.4
	24	OA/AO	0	17.56	19.8
	168	OA/AO	0	45.60	51.3
$Fe_3O_4-PEI-Au_{coat5}$	control	aqua regia	493.8	85.29	100.0
	1	OA/AO	0	0.15	0.2
	24	OA/AO	0	0.82	1.0
	168	OA/AO	0	0.95	1.1

for Au coating procedures in the aqueous phase,[8,37] and will require further refinement if particles are to be used in applications where a narrow size distribution of Au-coated particles is required. Comparisons with reported literature suggest that using monodispersed magnetic core particles could help to improve the monodispersity of final Au-coated particles using this coating procedure.[12] The use of Fe_3O_4 cores synthesized by other methods, however, could result in changes in the particle magnetic response or the ability to immobilize a dense layer of Au seeds on cores. Majetich and co-workers have previously highlighted the importance of the size difference between Au seeds and Fe_3O_4 cores in obtaining core−shell structures,[37] and we have found this to be the case when attempting to coat 10 nm Fe_3O_4 cores synthesized by an aqueous coprecipitation method.[38] It is likely that there will be a tradeoff between the key particle properties of monodispersity, magnetic response, and aggregation stability; this has to be considered when designing particles for specific applications.

Evidence of Au Coating. One of the criteria we believe to be important for the synthesis of Au-coated Fe_3O_4 is the completeness of Au coating. We considered the coating to be complete when all the Fe_3O_4 in each sample was coated with a protective layer of Au. This is important in applications where exposed Fe_3O_4 could dissolve leading to the degradation of particles and contamination of sample. To determine the completeness of our coating procedure, X-ray photoelectron spectroscopy (XPS) was first used to study the changes in surface composition of the particles as during each step in the fabrication process.

Analysis of the XPS spectra revealed the decrease in Fe peaks (Figure 6a) in tandem with the increase in Au peaks (Figure 6b). Quantitatively, the surface elemental atomic ratio of iron to gold changed from (i) 100:0 for Fe_3O_4 to (ii) 40:60 for $Fe_3O_4-PEI-Au_{seed}$ and finally to (iii) 7:93 for $Fe_3O_4-Au_{coat5}$. These results indicate the success in initial deposition and subsequent growth of Au on the Fe_3O_4 particles. The detection of Fe atoms after Au coating however had two possible implications: either the thickness of the Au coating was less than 5−10 nm,[39] or there were exposed areas of Fe_3O_4 on the $Fe_3O_4-Au_{coat5}$ surface.

In addition to the XPS measurements, particles at three stages of the coating process, Fe_3O_4, $Fe_3O_4-PEI-Au_{seed}$, and $Fe_3O_4-PEI-Au_{coat5}$, were subjected to an iron oxide dissolution process. Previous studies have shown that exposure of Fe_3O_4 particles to oxalate ions results in the formation of a water soluble iron−oxalate complex which allows for the complete dissolution Fe_3O_4 particles.[40] It was hypothesized that particles with a complete Au coating would protect the Fe_3O_4 cores, thus preventing their dissolution. The dissolution process involved the mixing of a 0.02 M oxalic acid and ammonium oxalate (OA/AO) solution with the particles for a period of seven days. ICP-OES was then used to determine the extent of Fe_3O_4 dissolution in the reaction mixture. Control samples of each particle type were prepared by completely dissolving the particles in aqua regia followed by ICP-OES analysis. This allowed us to comparatively determine the extent of Fe_3O_4 dissolution in each of the particle types. The ICP-OES elemental analysis in Table 3 showed that for bare Fe_3O_4 particles, similar iron concentrations were detected with the 1 h, 24 h, and control samples, indicating that particles were completely dissolved by the oxalate solution within an hour of mixing. The $Fe_3O_4-PEI-Au_{seed}$ and $Fe_3O_4-PE-Au_{coat5}$ particles, however, were found to be more resistant to oxalate complexation for up to an hour, which was attributed to the protective presence of Au. Analysis after 24 and 168 h showed that Fe had begun to leach out from $Fe_3O_4-PEI-Au_{seed}$ particles with 19.8 and 51.3%, respectively, of the total Fe (compared with controls)

(37) Lim, J.; Tilton, R. D.; Eggeman, A.; Majetich, S. A. *J. Magn. Magn. Mater.* **2007**, *311* (1), 78–83.
(38) Massart, R. *IEEE Trans. Magn.* **1981**, *17* (2), 1247–1248.
(39) Siegbahn, K. *Philos. Trans. R. Soc. London, Ser. A* **1970**, *268* (1184), 33–57.
(40) van Oorschot, I.; Dekkers, M. *Geophys. J. Int.* **2001**, *145*, 740–748.

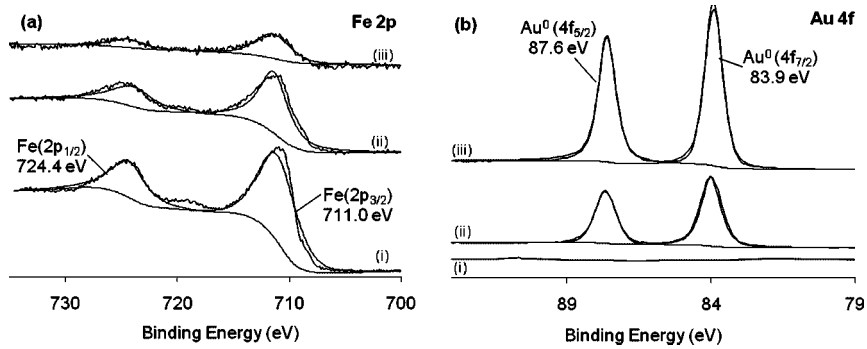

Figure 6. XPS spectrum and peak fit of the (a) Fe 2p and (b) Au 4f regions of (i) Fe_3O_4, (ii) $Fe_3O_4-PEI-Au_{seed}$, and (iii) $Fe_3O_4-PEI-Au_{coat5}$.

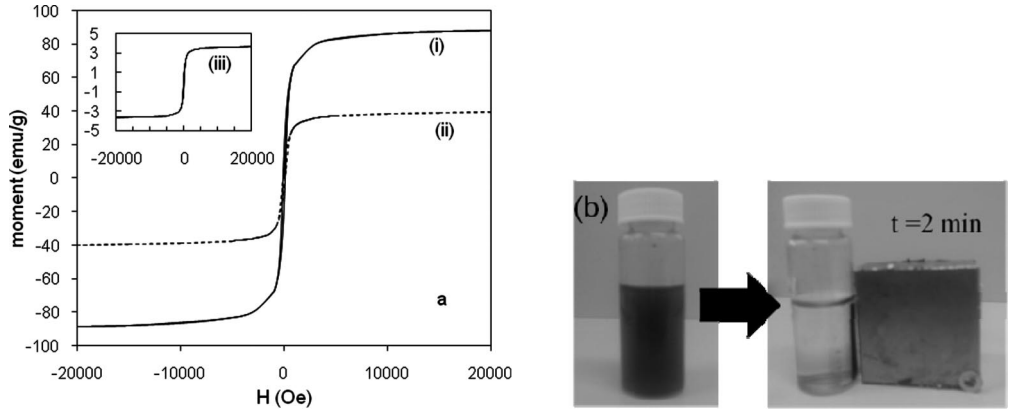

Figure 7. (a) SQUID magnetometry curves of (i) Fe_3O_4-PEI; (ii) $Fe_3O_4-PEI-Au_{seed}$ (iii) $Fe_3O_4-PEI-Au_{coat5}$ particles. (b) Behavior of $Fe_3O_4-PEI-Au_{coat5}$ particles under the influence of a magnetic field.

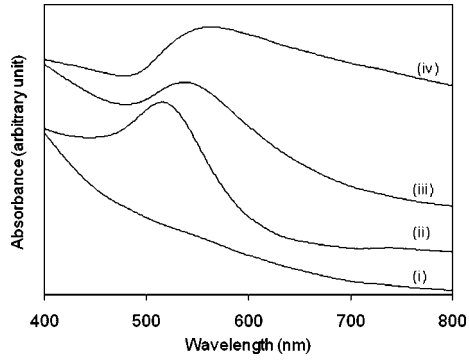

Figure 8. UV−vis spectra of (i) Fe_3O_4-PEI, (ii) Au seeds, (iii) $Fe_3O_4-PEI-Au_{seed}$, and (iv) $Fe_3O_4-PEI-Au_{coat5}$.

detected in solution. $Fe_3O_4-PEI-Au_{coat5}$ particles on the other hand, displayed excellent resistance to chemical dissolution with only 1% of the total Fe detected in solution even after 168 h of leaching. No further leaching was detected for the $Fe_3O_4-PEI-Au_{coat5}$ particles after 24 h compared to a 21% increase for the $Fe_3O_4-PEI-Au_{seed}$ particles after 168 h. The results obtained from XPS and oxalate dissolution where Au coating provides significantly enhanced protection compared to Au-seeded Fe_3O_4, suggests that that although the completeness of coating cannot be conclusively ascertained, the reported synthesis method allows for the deposition of a gold coating on Fe_3O_4 particles, which is akin to a complete shell for the time-scale of our experiments. STEM (scanning transmission electron microscope)/EDS (energy-dispersive spectroscopy) elemental maps performed in the TEM indicate that all areas in which Fe is detected, Au is also present (see Figure S3 in the Supporting Information). This suggests the successful immobilization of Au on every Fe_3O_4 particle. The limited resolution of this technique, however, means that it is unable to determine completeness of Au shell.

Effect of Au Coating on Magnetic Properties. The ability to manipulate synthesized particles using a magnetic field is the main driving force for utilizing Fe_3O_4 particles as the support for Au coating. It is thus important to characterize the effect of Au coating on the magnetic properties of the particles. Superconducting quantum interference device (SQUID) magnetization curves at 25 °C showed that saturation magnetization (M_s) of the Fe_3O_4-PEI particles (Figure 7a(i)) decreases as Au is loaded onto the particles. The decreases in magnetism were compared to the weight increases in Au and showed that 47% and 91% increase in weight of Au (Table 1) led to a 54 and 95% decrease in M_s, respectively (Figure 7a(ii) and 7a(iii)). The decrease in magnetism is therefore attributed mainly to the increase in weight ratio of Au to Fe_3O_4 due to the presence of Au on particles and is an unavoidable consequence of Au loading. A suspension of $Fe_3O_4-PEI-Au_{coat5}$ could, however, be separated by a neodymium magnet in 2 min (Figure 7b) showing that the particles maintain strong magnetism after Au coating. Attempts to redisperse the particles after magnetic separation show that although the particles are not superparamagnetic because of their size (>10 nm), the magnetic remanence (M_r) of the Au coated particles (~15% M_s) allows the particles to be easily redispersed in the absence of a magnetic field.

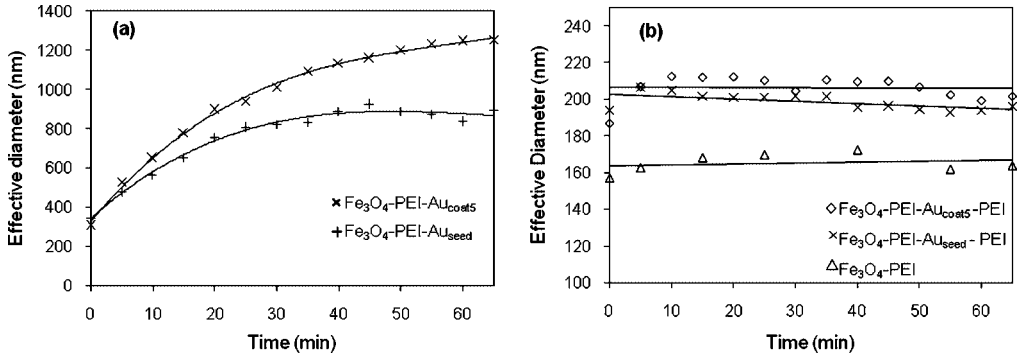

Figure 9. DLS measurements on (a) particles without PEI; (b) particles with PEI functionalization.

Effect of Au Coating on Optical Properties. Optical properties of particles with different Au loadings suspended in water were compared via UV−vis spectroscopy. Initial scans of Fe_3O_4−PEI particles produced featureless spectra indicating an absence of surface plasmon resonance (SPR) (Figure 8i). when a layer of Au seeds were attached onto Fe_3O_4 particles, a SPR peak developed at 550 nm (Figure 8iii), which was red-shifted and broader compared to the narrow peak at 520 nm observed for Au seed particles (Figure 8ii). Deposition of Au to form a coating resulted in further broadening of the peak which is also shifted to 580 nm (Figure 8iv). The initial emergence of a plasmon resonance peak was attributed to the presence of Au seed particles and Fe_3O_4 cores,[41] further broadening and shifting observed with the Fe_3O_4−PEI−Au_{coat5} particles was due to particle-to-particle interactions as a result of the higher packing density of the Au particles on the Fe_3O_4 surface after coating.[42]

PEI as an Effective Barrier to Aggregation. Earlier sections of this paper have focused on the utility of PEI as a functional layer on Fe_3O_4 particles, which allows for Au loading; however, a second important function of the PEI layer is to keep synthesized particles resistant to agglomeration and flocculation. Dynamic light scattering (DLS) measurements of the hydrodynamic (effective) diameters of the particles in a 10 mM NaCl background electrolyte at pH 7 to simulate a biological environment were used to study particle aggregation behavior up to 1 h after particles were subjected to sonication via an ultrasonic probe. (Figure 9).

It was observed that particles without PEI coatings (Figure 9a), including bare magnetite (not shown), began to aggregate immediately after sonication and hydrodynamic diameters increase to 1 μm, after which particles settle rapidly to the bottom of the cuvette. The PEI-coated particles however, show significantly enhanced stability against aggregation, with DLS hydrodynamic diameters remaining fairly constant at around 200 nm (Figure 9b). This stability is attributed to the electrostatic and steric repulsion between particles provided by the PEI. Particle resistance to aggregation is vital in this method of synthesis, as it ensures that during the coating process, only small Fe_3O_4 aggregates consisting of 1−4 particles are coated with Au rather than the coating of larger aggregates which would result in large Au-coated particles. PEI functionalization of gold-coated particles also ensures long-term (>1 week) stability of particles without sonication, which is important particularly for in vivo biological applications. The use of Au-coated Fe_3O_4 particles in a variety of applications will require surface functionalization with a range of different functional groups such as amine or carboxyl groups.[43] In such cases, the Au-coated Fe_3O_4 particles can be functionalized with non-polymeric molecules such as thiols. Such modifications affect the aggregation stability of the particles and have to be studied in the context of the intended application. Further study in this area is currently underway.

Differences between the TEM dimension histograms in Figure 2 and dynamic light scattering (DLS) "hydrodynamic diameters" in Figure 9 can be attributed to the differences in the measurement techniques. The TEM counting technique was used to determine primary particle size without taking into account aggregation of particles in solution; hence if particles do form aggregates of 2−3 particles, this would result in the increased dimensions observed via DLS. Another possible reason for the difference is that the calculation of hydrodynamic diameters takes into account the polymer coating and electric double layer (considerable for our highly charged particles) surrounding the particles in solution; this would result in an increased hydrodynamic diameter measured by DLS, a phenomena also observed by others.[44]

Conclusion

Presented in this study is a facile method of producing 50 to 150 nm gold−shell magnetite-core particles utilizing magnetite functionalized with polyethyleneimine. This stepwise, aqueous-based method performed at room temperature produces gold-coated magnetite particles that are magnetic and resistant to aggregation and are thus attractive for utilization in a wide range of biological applications. We demonstrate the importance of having a saturated surface of gold seeds in obtaining gold shells

(41) Averitt, R. D.; Sarkar, D.; Halas, N. J. *Phys. Rev. Lett.* **1997**, *78* (22), 4217–4220.
(42) Xu, X.; Cortie, M. B. *J. Phys. Chem. C* **2007**, *111* (49), 18135–18142.
(43) Zhao, X.; Cai, Y.; Wang, T.; Shi, Y.; Jiang, G. *Anal. Chem.* **2008**, *80* (23), 9091–9096.
(44) Meledandri, C. J.; Stolarczyk, J. K.; Ghosh, S.; Brougham, D. F. *Langmuir* **2008**, *24* (24), 14159–14165.

and also show that this shell imparts resistance to chemical attack. We also address the problems of poor magnetic strength, presence of uncoated particles, and complex, "nongreen" synthesis methods reported by related studies. In addition, this work highlights the utility of polyethyleneimine as a bridge to attach gold nanoparticles and coatings onto iron oxide surfaces, which could potentially be extended to a range of other surfaces and metallic nanoparticles.

Acknowledgment. The authors thank Joseph Horvart for performing SQUID measurements and the Australian Research Council for funding.

Supporting Information Available: Transmission electron micrographs and Scanning transmission electron microscope/energy-dispersive spectroscopy elemental maps (PDF). This material is available free of charge via the Internet at http://pubs.acs.org.

CM8025329